

CONTINUOUS VERTICAL PROFILES OF TEMPERATURE AND HUMIDITY AT LAMPEDUSA ISLAND

Pace Giandomenico⁽¹⁾, Cremona Giuseppe⁽⁴⁾, di Sarra Alcide⁽¹⁾, Meloni Daniela⁽¹⁾, Monteleone Francesco⁽²⁾, Sferlazzo Damiano⁽³⁾, Zanini Gabriele⁽⁴⁾

⁽¹⁾ Laboratory for Earth Observations and Analyses, ENEA. Via Anguillarese 301, 00123 Rome, Italy, Email: giandomenico.pace@enea.it, daniela.meloni@enea.it, alcide.disarra@enea.it

⁽²⁾ Laboratory for Earth Observations and Analyses, ENEA, Via Catania, 2 - 90141 Palermo, Italy, Email: francesco.monteleone@enea.it

⁽³⁾ Laboratory for Earth Observations and Analyses, ENEA, Loc. Capo grecale - 92010 Lampedusa, Agrigento, Italy, Email: damiano.sferlazzo@enea.it

⁽⁴⁾ Laboratory for Models, Methods and Technologies for the Environmental Assessment, ENEA, Via Martiri di Monte Sole, 4, 40129 Bologna, Italy, Email: gabriele.zanini@enea.it, giuseppe.cremona@enea.it

ABSTRACT

In May 2009 a microwave radiometer developed by Radiometer Physics GmbH (RPG), the Humidity And Temperature PROfiler (HATPRO), was installed at the ENEA Station for Climate Observations on the island of Lampedusa. Almost two years of vertical profiles of temperature and absolute humidity data are presented and discussed in terms of monthly mean and variability. Both temperature and absolute humidity profiles present a clear annual cycle characterized by thermally stable conditions and high values of absolute humidity from April to August, and by unstable temperature profiles and lower absolute humidity during the winter months. The vertical gradients of temperature reach a maximum value of about 0.8 K/km in July, while gradients of absolute humidity reach a minimum value of about $-9 \text{ g/m}^3\text{km}$ in September.

1. INTRODUCTION

Lampedusa (35.5°N, 12.6°E) is a small island of about 22 km² area, characterized by a plateau degrading from North to South, with the maximum elevation of 133 m. It is about 100 and 250 km from the Tunisian and the Sicilian coasts, respectively. The ENEA (the National Agency for New Technologies, Energy, and Sustainable Economic Development of Italy) Station for Climate Observation (www.lampedusa.enea.it) in Lampedusa is operational since 1998 and offers a unique opportunity to provide long time series of atmospheric parameters representative for the marine background conditions of the Mediterranean.

Measurements of several atmospheric parameters, such as greenhouse gases concentration, aerosol optical properties [1,2], radiative fluxes, column water vapour, meteorological variables, total ozone, UV irradiance [3, 4], and aerosol chemical composition [5] are carried out continuously. Continuous measurements of absolute humidity and temperature vertical profiles, integrated water vapour, liquid water content and cloud base height were started in May 2009 by means of a

HATPRO microwave radiometer (MWR). Measurements at Lampedusa were interrupted in the period September 2009 to November 2010, due to the participation of the MWR in the validation campaign of the MINNI air quality model (www.minni.org). The MWR was newly operational at Lampedusa in November 2010.

2. MEASUREMENTS

The HATPRO is installed on the roof of the station, close to the Northern edge of the Northern plateau, at an altitude of about 50 above the sea level. The MWR measures the brightness temperature at the high and low-frequency wings of the water vapour and of oxygen absorption bands, centered at 22.235 and 60 GHz, respectively. The instrument can operate looking at the vertical and/or in scanning mode; at Lampedusa, in the scanning mode, the HATPRO looks at 6 different elevation angles towards the sea to measure high resolution temperature profiles in the first 2 km. Further details on the instrument characteristics are available in [6].

Absolute calibration of all the channels is carried out using liquid nitrogen; due to the relatively high atmospheric transparency in the 22 GHz region, the sky tipping methodology is also used to calibrate the water vapour channels [7]. Thanks to the HATPRO high stability, starting from June 2011 also the water vapour channels were calibrated only using liquid nitrogen; these calibrations were made in July 2009, June, and September 2011. A statistical inversion methodology, similar to that described in [8] is used to derive column-integrated water vapour and liquid water path as well as profiles of temperature and specific humidity. Vertical profiles of specific humidity and temperature are calculated using quadratic and linear regressions, respectively. The coefficients used for the regressions were provided by RPG and derived on the basis of an ensemble of radiosounding data of the Mediterranean sites of Trapani and Cagliari.

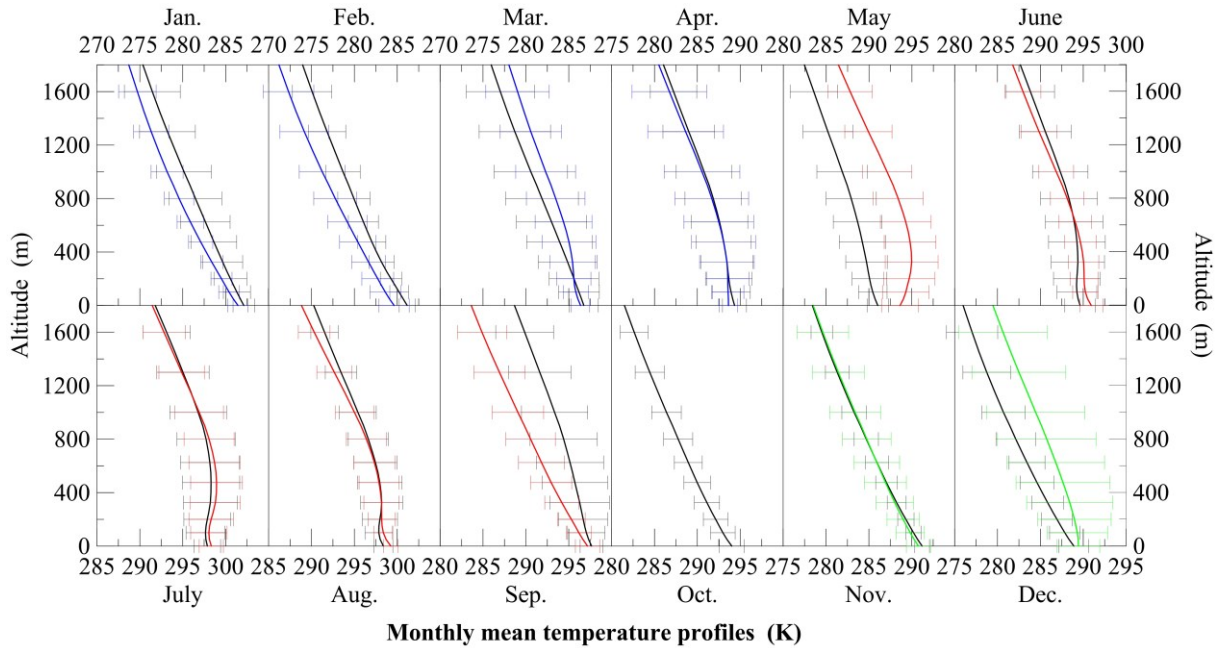


Figure 1. Monthly mean temperature profiles. Error bars represent one standard deviation. Red, green, black and blue lines refer to 2009, 2010, 2011, and 2012, respectively. Note the different horizontal scales.

Absolute humidity profiles are derived from observations to the vertical and have a nominal vertical resolution of 200 m from the surface to 2 km, and 400 m from 2 to 5 km, with an accuracy of 0.4 g/m³ RMS. Temperature profiles derived by scanning mode observations have a vertical resolution of 50 m from the surface to 1.2 km, and of 200 from 1.2 to 2 km, with a nominal accuracy of 0.25, 0.5 and 0.75 K from 0 to 500 m, from 500 to 1200m, and above 1200 m, respectively. With the exception of some short periods, the HATPRO has operated continuously in vertical mode, acquiring a vertical profile each minute, and in scanning mode once every 10-15 minutes.

The instrument is also provided by a rain sensor and an KT 19 II Heitronics infrared radiation pyrometer. These ancillary measurements provide useful information for the data analysis, especially in a very demanding environment such as that of Lampedusa. In fact, in spite of a fan and a supplementary heater, the formation of dew over the MWR hydrophobic radome may sometimes occur, degrading the quality of the water vapour line data.

3. DISCUSSION

Fig. 1 shows 23 monthly mean vertical profiles of temperature with the corresponding standard deviation, starting from June 2009 to April 2012. Averages are performed over all the data for which the rain sensor indicates absence of rain. This is a conservative

assumption because the rain sensor may indicate rain also in case of clear sky conditions, with very high humidity or after strong wind episodes, when sea salt aerosol can be deposited on the sensor. In most cases, however, the fan and the supplementary heater are sufficient to avoid the formation of water on the MWR radome. Monthly mean profiles for May and September display the largest year-to-year changes. This behaviour can be partially explained by the low number of measurements collected during the two months in 2009, when measurements were acquired only for 18 and 11 days for May and September respectively. The temperature profiles show a clear annual cycle characterized by variations in the vertical gradients, especially at the lowest altitudes.

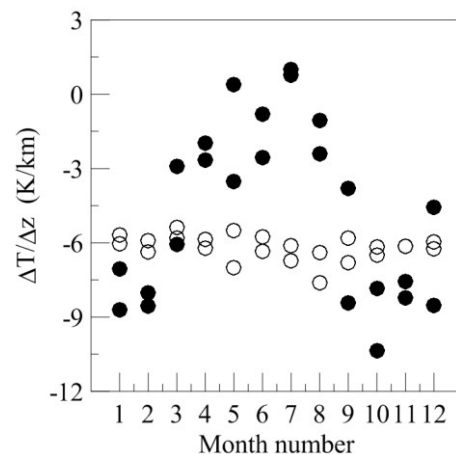


Figure 2. Monthly distribution of the temperature vertical gradient calculated from the surface to 700 m (black dots), and from 800 to 2000 m (open circles).

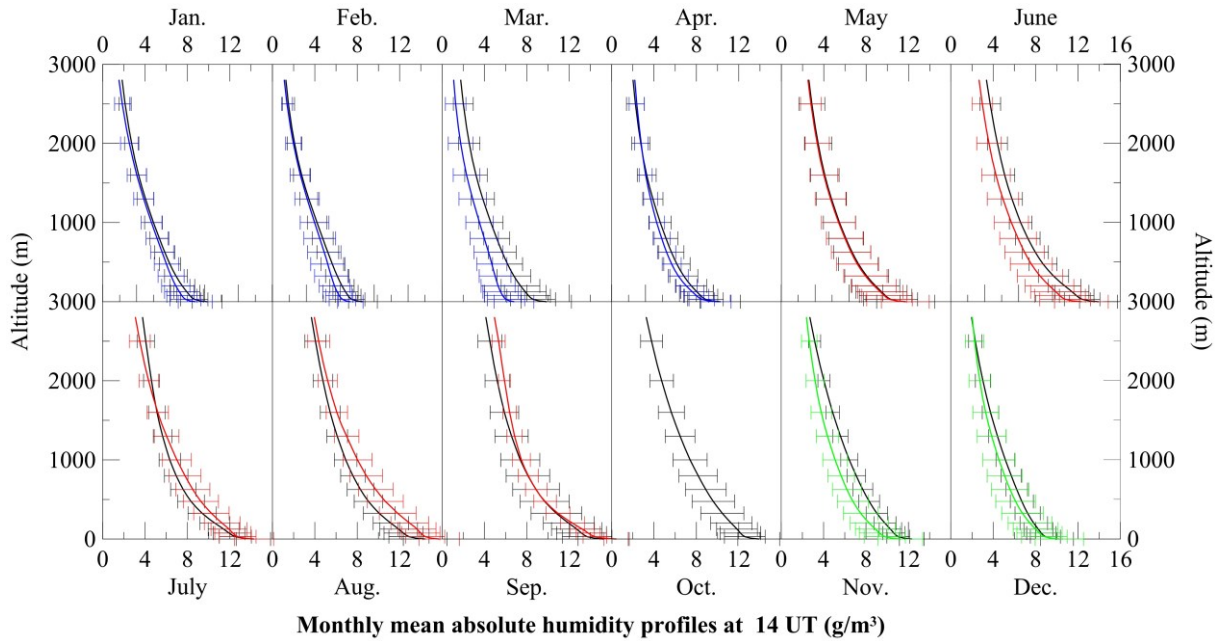


Figure 3. Monthly mean absolute humidity profiles. Error bars indicate one standard deviation. Red, green black and blue lines refer to months of 2009, 2010, 2011 and 2012 months, respectively.

Temperature inversions start in April, become a dominant phenomenon during the June, July, and August, and suddenly disappear in September. Temperature gradients were calculated from the surface to 700 m, and from 800 to 2000 m; their evolution is shown in Fig 2. Gradients were calculated by linear fits to temperature and altitude data. A well defined annual cycle is evident, with stable conditions from April to August and maxima around 0.8 K/km in July. Unstable conditions occur from October to February when the gradient may be as low as -8 K/km. As expected, gradients calculated between 800 and 2000 m do not display a clear annual cycle, and show values around -6 K/km.

Retrieved profiles of absolute humidity have lower vertical resolution than temperature, and are displayed over a larger range of altitudes, from 0 and 3000 m. To avoid contamination from wet radom cases, averages are calculated using data acquired between 14 and 15 UT (i.e. centered at 15:30 LT). Similarly to temperature, also the absolute humidity profiles show a clear annual cycle, with maximum surface values found between August and October and larger gradients in the lowest atmospheric layers during spring and summer. The annual course of the absolute humidity vertical gradient appears delayed by about 2 months with respect to temperature gradients (fig. 1 and fig.3). This behavior is highlighted by comparing fig. 4, where gradients of absolute humidity are presented, with fig. 2.

Similarly to temperature gradients, absolute humidity gradients have been calculated between the surface and 700 m, and from 800 and 3100 m. The absolute humidity vertical gradient in the lowest atmospheric layers show a very pronounced and regular cycle, with a minimum in August-September and a strong increase between September and October. The two month delay between the T and Q gradient cycles may be attributed to the different influence that the sea surface temperature (SST) induces on the two variables.

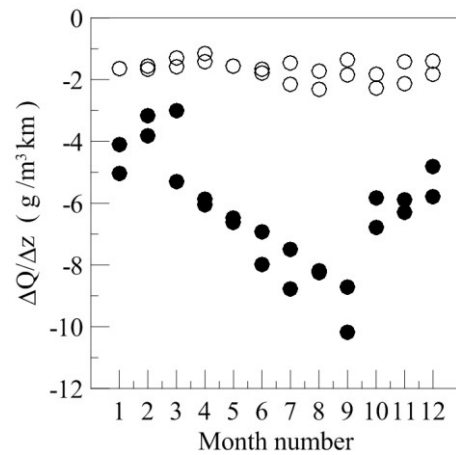


Figure 4. Monthly distribution of the absolute humidity gradient calculated from the surface to 700 m (black dots), and from 800 to 3100 m (open circles).

The delay in the annual warming of the SST with respect to the air temperature plays an important role in determining the temperature inversions in the lower atmospheric layers, leading to a rapid decrease of the temperature gradient absolute values in summer. The rapid change of air mass origin in September probably

plays a large role in determining the temperature vertical structure in early autumn.

Conversely, high SST may concur to the late summer increase of the humidity gradient, by facilitating the accumulation of large amounts of Q in the lowest layers.

4. CONCLUSIONS

Two year cycles of temperature and absolute humidity profiles measured at Lampedusa island have been presented and discussed. Both variables present a clear annual cycle. The monthly average profile suggest a larger thermal stability in the lower atmosphere in July; largest gradients of absolute humidity are observed in September. This shift is possibly due to the interaction between air and sea and to the differences between the annual cycle of air and sea surface temperature. This study confirms the potential of Lampedusa as a remote site for continuous measurement in the pristine maritime environment.

Acknowledgements. The authors thank the Radiometer Physics GmbH for providing instrumental and retrieval details for the HATPRO. This study was also conducted in the framework of the EG-CLIMET (ES0702) European COST action (<http://www.eg-climet.org>).

5. REFERENCES

1. di Sarra, A., Di Biagio, C., Meloni, D., Monteleone, F., Pace, G., Pugnaghi, S., and Sferlazzo, D. (2011) Shortwave and longwave radiative effects of the intense Saharan dust event of 25–26 March, 2010, at Lampedusa (Mediterranean sea), *J. Geophys. Res.*, **116**, D23209, doi:10.1029/2011JD016238, 2011.
2. Pace, G., di Sarra, A., Meloni, D., Piacentino, S., and Chamard, P. (2006). Aerosol optical properties at Lampedusa (Central Mediterranean). 1. Influence of transport and identification of different aerosol types, *Atmos. Chem. Phys.*, **6**, 697–713, doi:10.5194/acp-6-697-2006.
3. Meloni, D., di Sarra, A., Di Iorio, T., and Fiocco G. (2004). Direct radiative forcing of Saharan dust in the Mediterranean from measurements at Lampedusa island and MISR space-borne observations, *J. Geophys. Res.*, **109**, D08206, doi:10.1029/2003JD003960.
4. Di Biagio, C., di Sarra, A., and Meloni, D. (2010). Large atmospheric shortwave radiative forcing by Mediterranean aerosol derived from simultaneous ground-based and spaceborne observations, and dependence on the aerosol type and single scattering albedo, *J. Geophys. Res.*, **115**, D10209, doi:10.1029/2009JD012697.
5. Becagli, S., Sferlazzo, D. M., Pace, G., di Sarra, A., Bommarito, C., Calzolari, G., Ghedini, C., Lucarelli, F., Meloni, D., Monteleone, F., Severi, M., Traversi, R., and Udisti, R. (2012). Evidence for heavy fuel oil combustion aerosols from chemical analyses at the island of Lampedusa: a possible large role of ships emissions in the Mediterranean, *Atmos. Chem. Phys.*, **12**, 3479–3492, doi:10.5194/acp-12-3479-2012.
6. Rose, T., Crewell, S., Löhnert, U., Simmer, C. (2005). A network suitable microwave radiometer for operational monitoring of the cloudy atmosphere, *Atmos. Res.*, **75**(3), 183–200.
7. Han, Y. and Westwater, E. R. (2000). Analysis and Improvement of Tipping Calibration for Ground-Based Microwave Radiometers, *IEEE transactions on geoscience and remote sensing*, **38**(3), 1260–1276, doi:10.1109/36.843018
8. Löhnert, U., Crewell, S. (2003). Accuracy of cloud liquid water path from ground-based microwave radiometry: Part I. Dependency on cloud model statistics and precipitation. *Radio Sci.*, **38** (3), 8041.